Author Manuscript

Author Manuscript

Author Manuscript

Author Manuscript

HHS Public Access

Author manuscript

Life Sci. Author manuscript; available in PMC 2018 August 01.

Published in final edited form as:

Life Sci. 2017 August 01; 182: 41–49. doi:10.1016/j.lfs.2017.06.005.

Estrogen Receptor α Activation Enhances its Cell Surface Localization and Improves Myocardial Redox Status in Ovariectomized Rats

Rebecca J. Steagall, PhD[a], **Fanrong Yao, PhD**[a], **Saame Raza Shaikh, PhD**[b], and **Abdel A. Abdel-Rahman, PhD**[a,*]

[a]Department of Pharmacology and Toxicology, Brody School of Medicine, East Carolina University, Greenville, NC 27834, USA

[b]Department of Biochemistry and Molecular Biology, Brody School of Medicine, East Carolina University, Greenville, NC 27834, USA

Abstract

Aims—Little is known about the role of subcellular trafficking of estrogen receptor (ER) subtypes in the acute estrogen (E_2)-mediated alleviation of oxidative stress. We tested the hypothesis that ERα migration to the cardiac myocyte membrane mediates the acute E_2-dependent improvement of cellular redox status.

Main methods—Myocardial distribution of subcellular ERα, ERβ and G-protein coupled estrogen receptor (GPER) was determined in proestrus sham-operated (SO) and in ovariectomized (OVX) rats, acutely treated with E_2 (1 μg/kg) or a selective ERα (PPT), ERβ (DPN) or GPER (G1) agonist (10 μg/kg), by immunofluorescence and western blot. We measured ROS and malondialdehyde (MDA) levels, and catalase and superoxide dismutase (SOD) activities to evaluate myocardial antioxidant/redox status.

Key findings—Compared with SO, OVX rats exhibited higher myocardial ROS and MDA levels, reduced catalase and SOD activities, along with diminished ERα, and enhanced ERβ and GPER, localization at cardiomyocyte membrane. Acute E_2 or an ERα (PPT), but not ERβ (DPN) or GPER (G1), agonist reversed these responses in OVX rats and resulted in higher ERα/ERβ and ERα/GPER ratios at the cardiomyocytes membrane. PPT or DPN enhanced myocardial Akt phosphorylation. We present the first evidence that preferential aggregation of ERα at the cardiomyocytes plasma membrane is ERα-dependent, and underlies E_2-mediated reduction in oxidative stress, at least partly, via the enhancements of myocardial catalase and SOD activities in OVX rats.

*Corresponding Author: Dr. Abdel A. Abdel-Rahman, PhD, PAHA., Department of Pharmacology and Toxicology, Brody School of Medicine, East Carolina University, Greenville, NC 27834, USA, Tel: 252-744-3470 Fax: 252-744-3203, abdelrahmana@ecu.edu.

Disclosure of conflicts of interest

All of the authors declare that there are no conflicts of interest.

Publisher's Disclaimer: This is a PDF file of an unedited manuscript that has been accepted for publication. As a service to our customers we are providing this early version of the manuscript. The manuscript will undergo copyediting, typesetting, and review of the resulting proof before it is published in its final citable form. Please note that during the production process errors may be discovered which could affect the content, and all legal disclaimers that apply to the journal pertain.

Author Manuscript Author Manuscript Author Manuscript Author Manuscript

Significance—The findings highlight ERα agonists as potential therapeutics for restoring the myocardial redox status following E_2 depletion in postmenopausal women.

Keywords

estrogen receptor α; redox status; myocardium

1. Introduction

The favorable cardiovascular effects of estrogen (E_2) were questioned by findings of first Women's Health Initiative (WHI) study [1]. However, recent reappraisal of the WHI study showed that E_2 alone replacement therapy conferred cardioprotection in women aged 50–59 years [2]. The estrogen receptor (ER) subtype(s) mediation of E_2's cardiac effects [3–5] may involve many factors including: the subcellular location of the ERs, the interactions between the ER subtypes, and the timing of the response [6]. Currently, little is known about the role of ER subtypes and their subcellular trafficking in myocardial oxidative stress and its alleviation by E_2 replacement in menopausal women or in experimental models. Therefore, addressing these clinically relevant issues will advance our understanding of the protective cardiovascular effects of E_2 replacement.

Temporal and spatial aspects contribute to the complex nature of E_2 effects [7, 8]. E_2 binds to ERs, which continuously shuttle between various subcellular compartments, to produce their biological effects [9, 10]. There are three ER subtypes, which include the classical ERα and ERβ and the seven transmembrane-domain G-protein-coupled estrogen receptor (GPER). The latter also shuttles between the nucleus and the plasma membrane in response to E_2 [11, 12]. Activation of the docked ER at the plasma membrane [13–15] triggers signaling cascades that mediate the biological effects of E_2, such as activation of PI3K/Akt signaling [16] and regulation of vascular tone [17].

All three ER subtypes are expressed in the myocardium [18, 19], and are associated with the myocyte membrane [20] via caveolin-3 (Cav3) [21], a major component of lipid microdomains [22]. ERs interact with caveolins throughout the cardiovascular system [15, 23, 24], and acute E_2 enhances Cav3-ERα association on isolated rat cardiomyocytes cell surface [24]. However, there is little information on ERβ and GPER trafficking in cardiac myocytes following their acute activation with nonselective (E_2) or highly selective agonist for ERα (PPT) [25], ERβ (DPN) [26] or GPER (G1) [27]. Equally important, the functional relevance of such trafficking remains unknown. Functional crosstalk between the ER subtypes exists in various cell types including cancer [28, 29] and uterine epithelial [30] cells, but similar studies are lacking in cardiac myocytes. Interestingly, acute E_2 restores myocardial catalase activity of OVX rats to proestrus SO rats levels [31]. However, the implicated ER subtype in this latter effect remains unknown.

In the present study, we tested the hypothesis that E_2-mediated activation of ERα at the cardiomyocyte plasma membrane is pivotal for alleviating oxidative stress in OVX rats. Therefore, we investigated the distribution of subcellular ERα, ERβ and GPER protein levels and their level of colocalization with Cav3 in hearts collected from E_2-depleted (OVX) rats following acute administration of E_2 or a highly selective ERα (PPT), ERβ

Author Manuscript Author Manuscript Author Manuscript Author Manuscript

(DPN) or GPER (G1) agonist. Further, we investigated the effect of PPT on the cellular distribution of ERβ and GPER relative to ERα in OVX rats to gain more insight into role of ERα-dependent cellular trafficking in the acute E_2-mediated improvement of myocardial antioxidant/redox status in OVX rats [31].

2. Material and Methods

2.1. Animals

Female Sprague-Dawley rats (200–225 g, 12–13 weeks old, Charles River, Raleigh, NC) were housed two per cage in standard plastic cages, allowed free access to water and food (Prolab Rodent Chow; Granville Milling, Creedmoor, NC) and were maintained on a 12-12-hr light-dark cycle with lights off at 7:00 p.m. Room temperature was maintained at 23 ± 1°C, with humidity of 50 ± 10%. All experiments were carried out in accordance with, and approved by the East Carolina University Institutional Animal Care and Use Committee (AUP# W237) and in accordance with the Guide for the Care and Use of Laboratory Animals (Institute of Laboratory and Animal Resources, 2011).

2.2. Surgical preparation and ovariectomy

All surgeries were performed under aseptic conditions following anesthesia with intraperitoneal ketamine (90 mg/kg) and xylazine (10 mg/kg) injection as detailed in our recent study [32]. Each rat received subcutaneous injections of the analgesic buprenorphine hydrochloride (Buprenex, 30 μg/kg) and penicillin G benzathine and penicillin G procaine (Dura-Pen, 100,000 U/kg). Two weeks prior to intravascular cannulation for permit intravenous administration in conscious rats, bilateral ovaries were isolated and removed. Sham-operation (SO) was performed by exposing the ovaries without isolation.

2.3. Protocols and experimental groups

The hearts used in the present study were collected from rats used in our previous studies [31, 32]. Two weeks after ovariectomy, 5 groups of conscious OVX rats (n = 4–6) received a single injection of E_2 (1 μg/kg, i.v), a selective ERα (PPT), ERβ (DPN) or GPER (G1) agonist (10 μg/kg, i.v, each) or vehicle (saline). The hearts of the sixth group of SO rats, collected during the proestrus phase (highest endogenous plasma E_2 levels) evaluated by vaginal smear [33] served as controls. Plasma estradiol levels were evaluated in SO, OVX and OVXE2 rats. The doses of E_2 and the selective agonists were based on reported studies [34, 35], and the hearts were collected 90 min after drug or saline injection following euthanasia by over dose of phenobarbital, flash frozen in 2-methylbutane on dry ice, and stored at −80°C. ER subtype subcellular localization and biochemical studies (ROS and catalase activity) were conducted on these tissues as described below.

2.4. Quantitative colocalization microscopy

Spatial distribution of ERs, in relation to Cav3 was investigated by dual labeling immunofluorescence in heart sections as previously described [36]. Briefly, hearts were equilibrated to −20 °C and sectioned with a cryostat (HM 505E; Microm International GmbH, Waldorf, Germany). The heart tissue cryostat sections (20 μm thick) were post-fixed in 4% paraformaldehyde on Polysine® coated microscope slides (Thermo Scientific LLC,

Author Manuscript Author Manuscript Author Manuscript Author Manuscript

Portsmouth, NH) and blocked for 2 hrs with 10% normal donkey serum (Jackson Immunoresearch Laboratories, West Grove, PA) in Tris-buffered saline containing 0.2% Tween-20 (TBST). After overnight incubation with the primary antibody (1:50 dilution v/v), the sections were washed 3X with TBS, then incubated with the secondary antibody (1:150 dilution v/v) for 2 hrs and washed 1X with TBS containing 0.1% Triton-X. Coverslips were applied with Vectashield mounting medium with DAPI (Vector Laboratories, Inc., Burlingame, CA). Various combinations of the following primary antibodies were used for comparisons of subcellular localizations; mouse anti-ERα (Abcam, Cambridge, MA; ab2746), rabbit anti-ERα (Abcam; ab32063), mouse anti-ERβ (Abcam; ab16813), rabbit anti-ERβ (Abcam; ab3576), rabbit anti-GPR30 (Abcam; ab39742), mouse anti-Cav3 (BD Transduction Labs., San Jose, CA; 610421) and rabbit anti-Cav3 (Abcam; ab2912). The myocyte specific mouse anti-α-Actinin (Sarcomeric) antibody (Sigma Aldrich, St. Louis, MO, A7811) was used to verify that the sections analyzed were cardiomyocytes. The secondary antibodies used were: Cyanine3 (Cy3)-conjugated donkey anti-rabbit IgG (H+L) (Jackson ImmunoResearch; 711-165-152) and Fluorescein (FITC)-conjugated donkey anti-mouse IgG (H+L) (Jackson ImmunoResearch; 715-095-150). Control sections were incubated with only secondary antibodies to determine non-specific staining. A random sample of images across the heart section were acquired by laser scanning at wavelengths 488 and 543 nm using the Zeiss LSM 700 confocal microscope and the image analysis software ZEN 2012 (Carl Zeiss, Jena, Germany) keeping parameters constant throughout the acquisition process.

2.5. Colocalization image analysis

For colocalization quantification, we determined the fraction of ER that colocalized with Cav3 using the JACoP plug in for NIH ImageJ (http://rsbweb.nih.gov/ij/) as previously described [37]. Briefly, the degree of colocalization between the fluorophores ER-FITC (green) with Cav3-Cy3 (red) in the confocal images was quantified after background subtraction using Pearson's correlation coefficient (P_r), which performs intensity correlation coefficient-based (ICCB) analyses [38]. Further, the colocalization threshold tool was used to visualize the corresponding scatter plots of colocalization in NIH ImageJ. The values range from 1 to −1 indicating full positive and negative correlation, respectively, while zero indicates no correlation [38]. For all measurements, we collected four to six images from four to six separate experiments.

2.6. ER plasma membrane ratios

The ERα/ERβ and ERα/GPER plasma membrane ratios were quantified using the following equations:

$$\frac{\mathrm{PrER}\alpha,\mathrm{Cav3}}{\mathrm{PrER}\beta,\mathrm{Cav3}} \quad \frac{\mathrm{PrER}\alpha,\mathrm{Cav3}}{\mathrm{PrGPER},\mathrm{Cav3}}$$

Where P_r ERα, Cav3 is Pearson's correlation coefficient of ERα with Cav3, and P_r ERβ, Cav3 and P_rGPER, Cav3 are Pearson's correlation coefficients of ERβ and GPER with Cav3, respectively.

Author Manuscript Author Manuscript Author Manuscript Author Manuscript

2.7. Western blot analysis

Subcellular heart protein lysates of membrane, cytoplasmic and nuclear extracts were prepared using the Subcellular Protein Fractionation kit for tissues (Thermo Scientific, Pierce Biotechnology, Rockford, IL). Equal amounts of proteins (30 μg) were resolved by 10% SDS–PAGE and semi-dry transferred to nitrocellulose membranes (BIO-Rad), which undergone blocking for 2 hrs with Odyssey Blocking Buffer (LI-COR Biosciences, Lincoln, NE), then probed overnight at 4°C with a mixture of ERα (1:500, Abcam, Cambridge, MA), NA/K ATPase (1:2000, Abcam, Cambridge, MA), β-actin (1:5000, Abcam), and Laminin B (1:2000, Santa Cruz Biotechnology, Santa Cruz, CA) antibody, respectively. The membranes were then incubated for 60 min with a mixture containing IRDye680-conjugated goat anti-mouse and IRDye800-conjugated goat anti-rabbit (1:15,000, LI-COR Biosciences). Bands were detected by Odyssey Infrared Imager and quantified by integrated intensities with Odyssey application software version 5.2 (LI-COR Biosciences).

2.8 ROS measurement

Fresh unfixed heart sections (20 μm) were incubated with 10 μM dihydroethidium (DHE, Molecular Probes, Grand Island, NY) at 37 °C in the presence of 5% CO_2 in a moist chamber for 30 min. Negative controls were used to determine non-specific staining. Images were visualized with a Zeiss LSM700 microscope. Four to six images were acquired from four to six heart sections for each experimental condition. After background subtraction, quantification of the fluorescent ethidium signal was conducted using ImageJ software (NIH) and changes in total fluorescence intensity were calculated as reported [39].

2.9. Catalase activity assay

The commercially available colorimetric catalase assay kit from Sigma-Aldrich (St. Louis, MO) was used to measure catalase activity in 10 μg protein of ventricular homogenates according to the manufacturer's instructions and our recent study [31].

2.10. Superoxide dismutase (SOD) activity assay

Myocardial SOD activity was measure by EnzyChrom Super Dismutase Assay Kit (EROD-100, BioAssay Systems, Hayward, CA) following the manufacturer's instructions.

2.11 Malondialdehyde (MDA) levels

TBARS Assay Kit (Cayman Chemical, Ann Arbor, MI, USA) was used to measure myocardial MDA level following the manufacturer's protocol and the method descripted in our publication [40]. The MDA-TBA adduct was detected colorimetrically at 530–540 nm.

2.12 Determination of plasma 17β-estradiol

2.12 Plasma E_2 levels

Blood samples were collected from the artery catheter before hemodynamic experiment, centrifuged at 4000 rpm, 4°C for 10 min. The plasma was separated and stored at −20 °C. The estradiol level in the samples was measured with ELISA immunoassay (Estradiol EIA kit, Oxford Biomedical Research, Oxford, MI) according to manufacturer's instructions [41].

Author Manuscript Author Manuscript Author Manuscript Author Manuscript

2.13. Drugs

Ketamine and xylazine were purchased from Phoenix Pharmaceuticals Inc., (St Joseph, MI). Buprenorphine was purchased from Rickitt & Colman (Richmond, VA). Dura-Pen was from Vedco Inc. (Overland Park, KS). 17β-estradiol sulfate, Propylpyrazole triol (PPT) and 2,3-bis(4-hydroxyphenyl)-proprionitrile (DPN) were purchased from Sigma Aldrich (St. Louis, MO). G1 was purchased from Tocris Biosciences (Ellisville, MO). The ER agonists were dissolved in DMSO for stock solution and the working concentration was a 1:50 dilution in sterile saline. Sterile saline was purchased from B. Braun Medical (Irvine, CA).

2.14. Statistical analysis

DHE fluorescence intensity, catalase activity, receptor subtype plasma membrane ratios, and fluorescence colocalization (P_r) values were grouped, analyzed for normal distribution using one-way ANOVA with post hoc comparisons (HOLM-Sidak test) and presented as mean ± SEM. Correlation coefficients were obtained for ER plasma membrane ratios versus catalase activity using Pearson Product-Moment correlation measurements [42]. Western blot data was expressed as fold change versus OVX (saline) values and analyzed by unpaired *t*-test or ANOVA. Probability values (*P*) of < 0.05 were considered to be significant. All statistical analyses were conducted using Origin 8.5 (OriginLab, Northampton, MA) or Sigmastat 3.1 (Systat, San Jose, CA) software.

3. Results

3.1. Acute E_2 enhances ERα, reduces ERβ and GPER, localization at the cardiac myocyte membrane in OVX rats

Compared with SO rats, ovaryectomy significantly reduced the plasma E_2 level and acute E_2 (1 μg/kg) administration restored the E_2 level in OVX rats (Supplemental Figure 1). The relative colocalization of ERα, ERβ or GPER with Cav3 at the cardiac myocyte membrane revealed significant ($P < 0.05$) reduction in ERα, and elevations in ERβ and GPER, localization at the plasma membrane in OVX, compared with SO rats. Acute E_2 (1 μg/kg) administration restored these patterns to those observed in SO rats (Fig. 1). Therefore, E_2 depletion reduced ($P < 0.05$) the ERα/ERβ (Fig. 2A) and ERα/GPER (Fig. 2B) ratios at cell membrane, a phenomenon that was reversed by acute E_2 administration (Fig. 2). Staining with the myocyte specific antibody, anti-α-actinin (Sarcomeric) antibody, confirmed that these responses occurred in cardiomyocytes (Supplemental Fig. 2A). The inclusion of negative controls validated the specificity of the antibodies used in our study (Supplemental Fig. 2B). E_2 also caused ERα translocation to plasma membrane (Supplemental Fig. 2C) and ERβ to the nuclei (DAPI stained, Supplemental Fig. 2D).

3.2. Selective activation of ERα, ERβ or GPER replicates the effect of E_2 on ER subtype localization at the cardiac myocyte plasma membrane in OVX rats

Based on the relative localization of ERα, ERβ or GPER with Cav3 in the myocytes plasma membrane (Figs. 3A, B and C), OVX rats exhibited higher ($P < 0.05$) ratios of ERβ/Cav3 and GPER/Cav3 than ERα/Cav3 (Fig. 3D). Acute administration of a selective agonist (10

Author Manuscript Author Manuscript Author Manuscript Author Manuscript

μg/kg) for ERα (PPT) enhanced ($P < 0.05$), while ERβ (DPN) or GPER (G1) reduced ($P < 0.05$), the localization of the targeted ER subtype at the plasma membrane (Fig. 3).

To corroborate the immunofluorescence findings (Figs. 1–3), we conducted Western blot analyses on myocardial membrane, cytoplasmic and nuclear fractions. Acute E_2 (1 μg/kg) significantly ($P < 0.05$) enhanced and reduced ERα protein level in the plasma membrane and cytoplasmic fractions, respectively, but had no effect on the ERα protein level in the nuclear fraction (Fig. 4).

3.3. ERα plays a pivotal role in the E_2 mediated amelioration of oxidative stress

Compared with proestrus SO levels, OVX rats exhibited significantly ($P < 0.05$) higher myocardial ROS (Fig. 5) and MDA (Fig. 6D) level ($P < 0.05$). These responses were reversed ($P < 0.05$) by acute E_2 (1 μg/kg) or PPT (10 μg/kg), but not by DPN or GPER (Figs. 5 and 6). Pearson Product-Moment Correlation analysis of data generated in OVX with and without E_2 showed inverse relationships (Figs. 5C and D) between cardiac ROS levels and plasma membrane ratios of ERα/ERβ ($r = -0.817$; $P < 0.05$) or ERα/GPER ($r = -0.762$; $P < 0.05$).

3.4. ERα mediates E_2-evoked enhancements of myocardial catalase and SOD activities, as well as Akt phosphorylation in OVX rats

OVX rats exhibited reduced ($P < 0.05$) myocardial catalase (Fig. 6A) and SOD (Fig. 6C) activities, compared with SO rats. E_2 or PPT, but not DPN or G1, restored the activities of both enzymes to SO levels although E_2 was more effective in this regards (Fig. 6A, C). Pearson Product-Moment Correlation analysis of data generated in OVX with and without E_2 showed positive relationships between catalase activity and the plasma membrane ratios of ERα/ERβ ($r = 0.922$; $P < 0.05$) or ERα/GPER ($r = 0.822$; $P < 0.05$) (Figs. 6B and C). Finally, PPT or DPN increased ($P < 0.05$), while G1 had no effect on, the phosphorylation of the survival molecule AKt in the myocardium of OVX rats (Fig. 7).

4. Discussion

The current study contributes the following new knowledge on E_2 modulation of subcellular distribution and function of the three ER subtypes in cardiomyocyte. Compared to proestrus SO rats, a drastic reduction in ERα/ERβ or ERα/GPER ratio at the cardiac myocyte membrane in OVX rats, was associated with myocardial oxidative stress and reduced catalase activity. Acutely administered E_2 restored ERα/ERβ and ERα/GPER ratios to the levels in proestrus rats by concomitantly enhancing ERα, and reducing ERβ and GPER, localization at the myocyte membrane in OVX rats. Only PPT replicated these E_2-mediated effects in OVX rats suggesting a pivotal role for ERα in the preferential regulation of ER subtype translocation to, and from, its subcellular locales. This E_2- or PPT-dependent restoration of the ERα aggregation at the cell membrane is physiologically implicated in the E_2 antioxidant effect. This premise is supported by an ERα-dependent restoration of catalase and SOD activities and reduction of oxidative stress (ROS and MDA levels) in the myocardium of OVX rats.

Author Manuscript Author Manuscript Author Manuscript Author Manuscript

Our finding on the relative cellular distribution of the individual ER subtype in the cardiac myocytes of proestrus SO and OVX rats support a preferential E_2-driven ERα aggregation at the myocyte plasma membrane (Figs. 1–3). This premise was supported by variations in ERα protein distribution (western blot) in subcellular compartments in E_2 depleted (OVX) and replete ($OVXE_2$) rats. We show in OVX rats that acute E_2 administration increased and reduced ERα level in the plasma membrane, and cytoplasmic fraction, respectively, but had no effect on ERα protein level in nuclear extract (Fig. 4) or nucleus (Supplemental Fig. 2C). Interestingly, E_2 reduced ERβ level at plasma membrane (Fig. 1C, D), at least partly, by enhancing its translocation to the nucleus (Supplemental Fig. 2D). The translocation of a specific ER subtype might be tissue specific or time dependent. First, similar to our findings, short-term (minutes) exposure to 17β-estradiol increased the localization of ERα at plasma membrane of female rat anterior pituitary cell culture [43], while a longer time (2 hrs) was needed for ERα translocation to the nucleus in cancer cells [44]. Second, E_2 induces rapid ERβ translocation to the membrane of rat primary-cultured cortical neurons [45]. More studies are needed to determine the time-dependence of ERα distribution within the different cellular components of the cardiac myocyte.

We adopted colocalization analysis using confocal images, which permitted visualization (Figs. 1A, C and E) and quantification (Figs. 1B, D and F) of ER subtype association with the plasma protein Cav3. It is important to comment on the impact of E_2 depletion (OVX) on the spatial distribution of the three ER subtypes in the cardiac myocyte relative to such distribution in E_2 replete conditions, particularly during the proestrus phase, which exhibits the highest endogenous E_2 level [33]. We found that the heart of OVX rat exhibited reduced ERα (Fig. 1B), and enhanced ERβ (Fig. 1D) and GPER (Fig. 1F), localization at the plasma membrane of cardiac myocyte. Therefore, in the presence of endogenous E_2, ERα localization to the cardiac myocyte membrane (Fig. 1B) occurs at the expense of ERβ (Fig. 1D) and GPER (Fig. 1F). Interestingly, homo- or heterodimer formation of the two ER subtypes, ERα and ERβ, can form at the membrane as the main component of a signaling complex, and is required for rapid signaling [10, 46]. In the case of nuclear E_2 action, ERβ often has the opposite effect of ERα [47, 48]. The membrane GPER interactions with the ER subtypes can also influence E_2-mediated responses [28, 49]. It is likely that these 'Yin-Yang' relationships between the ER subtypes are influenced by the proportion of the ER subtypes available at the plasma membrane. Overall, the biological relevance of these endogenous E_2 driven plasma membrane ratios of the ER subtypes has not been seriously considered in reported studies.

We have shown that the reduction in myocardial catalase activity in OVX rats is restored to proestrus rat levels within minutes after E_2 administration [31] or selective ERα activation [32]. Further, we showed that acute ERα blockade by its selective antagonist MPP significantly reduced myocardial catalase activity in proestrus rats [40]. Collectively, these pharmacological findings support ERα mediation of cardiac catalase activation by acute or circulating E_2. The current findings (Fig. 6A) support this premise. Next, consistent with the premise that the spatial distribution of a protein plays a critical role in its function [50], we present the first evidence that the aggregation of the ERα at the cell membrane is critical for its mediation of: (i) the enhancement of catalase activity (Figs. 6B and C), and (ii) the suppression of ROS (Fig. 5) and MDA (Fig. 6D) levels in the OVX rat myocardium. ROS

Author Manuscript Author Manuscript Author Manuscript Author Manuscript

measurement was validated by two different assays in accordance with recent guidelines for ROS measurements [51]. However, it was important to determine if that the activation of ERα alone is enough to trigger the spatial distribution of the ERs in analogous manner to that caused by the endogenous hormone, E_2.

We show, for the first time, that acute administration of the selective ERα agonist PPT produced similar biochemical response (Figs. 5 and 6) and ER subtype distribution pattern (Fig. 2) to those produced by E_2 in OVX rats. Equally compelling are the findings that the selective ERβ or GPER activation produced opposite effect to those produced by E_2 or by PPT because DPN or G1 suppressed myocardial catalase activity (Fig. 6A) and did not reverse oxidative stress in OVX rats (Fig. 5). These novel findings set forth the postulate that activation of ERs by E_2 triggers concomitant dissociation of ERβ and GPER from the myocyte plasma membrane consequent to the enhanced translocation of ERα to the plasma membrane. These ER trafficking events seem to contribute to the E_2-dependent homeostasis within the rat myocardium because the predominance of ERα at the cardiac myocyte plasma membrane and its activation explain, at least partly, the acute antioxidant effect of E_2 (reduced ROS and MDA while enhancing myocardial catalase and SOD activities) in our model system.

These current findings are important because enhancement of cardiac catalase activity alleviates myocardial oxidative in E_2 treated OVX rats [52], and changes in cellular ER subtype ratios are linked to oxidative stress and antioxidant enzyme activity [53, 54]. Further, similar E_2 beneficial effects on the redox status were reported in female aortas and cardiac tissues [55, 56], and catalase supplementation is linked to improvements in functional recovery of globally ischemic and perfused isolated hearts [57]. It is imperative to consider the contribution of other antioxidant enzymes to the ERα-dependent improvement of the myocardial redox status such as mitochondrial aldehyde dehydrogenase (mitALDH2) because it contributes to the antioxidant effect of E_2 [58]. Nonetheless, the present findings support a role for ERα signaling mechanisms in the cardiovascular protective effect of acute E_2.

It is important to comment on the inability of selective ERα activation (PPT) to produce higher increases in catalase and SOD activities than that produced by E_2 in OVX rats. This was expected because the activities of both enzymes were suppressed following ERβ or GPER activation in OVX rats (Fig. 6A, C). These findings are consistent with a down-regulatory crosstalk where activated ERs can balance the net E_2-mediated response through opposing influences. In support of this notion, PPT replicated E_2-evoked dissociation of ERβ or GPER from plasma membrane (Figs. 1D and F). We must also consider the possibility that a crossover activation of the other ER subtype(s) by the selective agonists used in our study may have confounded data interpretation. This possibility is unlikely because, at the selected dose level, the agonists used in the present study are highly selective to their respective ER subtype; for example, PPT exhibits 400 fold preference to ERα and DPN exhibits 70 fold preference to ERβ and G1 is highly selective for GPER [25–27]. Therefore, the substantial selectivity of the utilized ER agonist, particularly the ERα agonist PPT, and the unique trafficking and biological activity of the ERα lend credence to our pharmacological approach and the novel data generated in our model system.

Author Manuscript Author Manuscript Author Manuscript Author Manuscript

5. Conclusion

The current study provides important mechanistic information on the role of ER subtype trafficking in regulating the redox status of the rat myocardium. Specifically, the acute E_2-mediated reversal of myocardial oxidative stress in E_2 depleted (OVX) rats is dependent on preferential ERα association with the myocyte cell membrane. Consistent with findings in other model systems [29, 48], our data support the involvement of a crosstalk among the ER subtypes. While both PPT and DPN enhanced the phosphorylation of the survival molecule Akt (Fig. 7), our novel findings support the hypothesis that ERα exhibits an additional function of triggering its translocation to the plasma membrane of cardiac myocyte. The latter seems to limit oxidative stress, at least partly, via enhancement of myocardial catalase and SOD activities. Finally, the findings highlight ERα agonists as potential therapeutics for restoring the myocardial redox status in postmenopausal women.

Supplementary Material

Refer to Web version on PubMed Central for supplementary material.

Acknowledgments

Funding

This work was partly supported by the National Institutes of Health [grant numbers R01 AA014441-10, AAA].

The authors thank Ms. Kui Sun for her technical assistance.

References

1. Rossouw JE, Anderson GL, Prentice RL, LaCroix AZ, Kooperberg C, Stefanick ML, et al. Risks and benefits of estrogen plus progestin in healthy postmenopausal women: principal results From the Women's Health Initiative randomized controlled trial. Jama. 2002; 288:321–33. [PubMed: 12117397]
2. Manson JE, Chlebowski RT, Stefanick ML, Aragaki AK, Rossouw JE, Prentice RL, et al. Menopausal hormone therapy and health outcomes during the intervention and extended poststopping phases of the Women's Health Initiative randomized trials. Jama. 2013; 310:1353–68. [PubMed: 24084921]
3. Kim JK, Levin ER. Estrogen signaling in the cardiovascular system. Nuclear receptor signaling. 2006; 4:e013. [PubMed: 16862219]
4. Wang F, He Q, Sun Y, Dai X, Yang XP. Female adult mouse cardiomyocytes are protected against oxidative stress. Hypertension. 2010; 55:1172–8. [PubMed: 20212261]
5. Deschamps AM, Murphy E. Activation of a novel estrogen receptor, GPER, is cardioprotective in male and female rats. American journal of physiology Heart and circulatory physiology. 2009; 297:H1806–13. [PubMed: 19717735]
6. Vrtacnik P, Ostanek B, Mencej-Bedrac S, Marc J. The many faces of estrogen signaling. Biochemia medica. 2014; 24:329–42. [PubMed: 25351351]
7. Soltysik K, Czekaj P. Membrane estrogen receptors - is it an alternative way of estrogen action? Journal of physiology and pharmacology: an official journal of the Polish Physiological Society. 2013; 64:129–42. [PubMed: 23756388]
8. Levin ER. Integration of the extranuclear and nuclear actions of estrogen. Molecular endocrinology. 2005; 19:1951–9. [PubMed: 15705661]

Author Manuscript Author Manuscript Author Manuscript Author Manuscript

9. Huang A, Sun D, Wu Z, Yan C, Carroll MA, Jiang H, et al. Estrogen elicits cytochrome P450--mediated flow-induced dilation of arterioles in NO deficiency: role of PI3K-Akt phosphorylation in genomic regulation. Circulation research. 2004; 94:245–52. [PubMed: 14670845]
10. Guo X, Razandi M, Pedram A, Kassab G, Levin ER. Estrogen induces vascular wall dilation: mediation through kinase signaling to nitric oxide and estrogen receptors alpha and beta. The Journal of biological chemistry. 2005; 280:19704–10. [PubMed: 15764600]
11. Cheng SB, Graeber CT, Quinn JA, Filardo EJ. Retrograde transport of the transmembrane estrogen receptor, G-protein-coupled-receptor-30 (GPR30/GPER) from the plasma membrane towards the nucleus. Steroids. 2011; 76:892–6. [PubMed: 21354433]
12. Pupo M, Vivacqua A, Perrotta I, Pisano A, Aquila S, Abonante S, et al. The nuclear localization signal is required for nuclear GPER translocation and function in breast Cancer-Associated Fibroblasts (CAF s). Molecular and cellular endocrinology. 2013; 376:23–32. [PubMed: 23748028]
13. Kelly MJ, Levin ER. Rapid actions of plasma membrane estrogen receptors. Trends in endocrinology and metabolism: TEM. 2001; 12:152–6. [PubMed: 11295570]
14. Razandi M, Oh P, Pedram A, Schnitzer J, Levin ER. ERs associate with and regulate the production of caveolin: implications for signaling and cellular actions. Molecular endocrinology. 2002; 16:100–15. [PubMed: 11773442]
15. Kim HP, Lee JY, Jeong JK, Bae SW, Lee HK, Jo I. Nongenomic stimulation of nitric oxide release by estrogen is mediated by estrogen receptor alpha localized in caveolae. Biochemical and biophysical research communications. 1999; 263:257–62. [PubMed: 10486286]
16. Wu KL, Chen CH, Shih CD. Nontranscriptional activation of PI3K/Akt signaling mediates hypotensive effect following activation of estrogen receptor beta in the rostral ventrolateral medulla of rats. Journal of biomedical science. 2012; 19:76. [PubMed: 22897791]
17. Haas E, Bhattacharya I, Brailoiu E, Damjanovic M, Brailoiu GC, Gao X, et al. Regulatory role of G protein-coupled estrogen receptor for vascular function and obesity. Circulation research. 2009; 104:288–91. [PubMed: 19179659]
18. Grohe C, Kahlert S, Lobbert K, Stimpel M, Karas RH, Vetter H, et al. Cardiac myocytes and fibroblasts contain functional estrogen receptors. FEBS letters. 1997; 416:107–12. [PubMed: 9369244]
19. Kvingedal AM, Smeland EB. A novel putative G-protein-coupled receptor expressed in lung, heart and lymphoid tissue. FEBS letters. 1997; 407:59–62. [PubMed: 9141481]
20. Chung TH, Wang SM, Wu JC. 17beta-estradiol reduces the effect of metabolic inhibition on gap junction intercellular communication in rat cardiomyocytes via the estrogen receptor. Journal of molecular and cellular cardiology. 2004; 37:1013–22. [PubMed: 15522278]
21. Song KS, Scherer PE, Tang Z, Okamoto T, Li S, Chafel M, et al. Expression of caveolin-3 in skeletal, cardiac, and smooth muscle cells. Caveolin-3 is a component of the sarcolemma and co-fractionates with dystrophin and dystrophin-associated glycoproteins. The Journal of biological chemistry. 1996; 271:15160–5. [PubMed: 8663016]
22. Li C, Duan W, Yang F, Zhang X. Caveolin-3-anchored microdomains at the rabbit sarcoplasmic reticulum membranes. Biochemical and biophysical research communications. 2006; 344:1135–40. [PubMed: 16647041]
23. Chambliss KL, Yuhanna IS, Mineo C, Liu P, German Z, Sherman TS, et al. Estrogen receptor alpha and endothelial nitric oxide synthase are organized into a functional signaling module in caveolae. Circulation research. 2000; 87:E44–52. [PubMed: 11090554]
24. Chung TH, Wang SM, Liang JY, Yang SH, Wu JC. The interaction of estrogen receptor alpha and caveolin-3 regulates connexin43 phosphorylation in metabolic inhibition-treated rat cardiomyocytes. The international journal of biochemistry & cell biology. 2009; 41:2323–33. [PubMed: 19523531]
25. Stauffer SR, Coletta CJ, Tedesco R, Nishiguchi G, Carlson K, Sun J, et al. Pyrazole ligands: structure-affinity/activity relationships and estrogen receptor-alpha-selective agonists. Journal of medicinal chemistry. 2000; 43:4934–47. [PubMed: 11150164]
26. Meyers MJ, Sun J, Carlson KE, Marriner GA, Katzenellenbogen BS, Katzenellenbogen JA. Estrogen receptor-beta potency-selective ligands: structure-activity relationship studies of

Author Manuscript Author Manuscript Author Manuscript Author Manuscript

diarylpropionitriles and their acetylene and polar analogues. Journal of medicinal chemistry. 2001; 44:4230–51. [PubMed: 11708925]

27. Bologa CG, Revankar CM, Young SM, Edwards BS, Arterburn JB, Kiselyov AS, et al. Virtual and biomolecular screening converge on a selective agonist for GPR30. Nature chemical biology. 2006; 2:207–12. [PubMed: 16520733]
28. Albanito L, Madeo A, Lappano R, Vivacqua A, Rago V, Carpino A, et al. G protein-coupled receptor 30 (GPR30) mediates gene expression changes and growth re sponse to 17beta-estradiol and selective GPR30 ligand G-1 in ovarian cancer cells. Cancer research. 2007; 67:1859–66. [PubMed: 17308128]
29. Zhao C, Matthews J, Tujague M, Wan J, Strom A, Toresson G, et al. Estrogen receptor beta2 negatively regulates the transactivation of estrogen receptor alpha in human breast cancer cells. Cancer research. 2007; 67:3955–62. [PubMed: 17440111]
30. Gao F, Ma X, Ostmann AB, Das SK. GPR30 activation opposes estrogen-dependent uterine growth via inhibition of stromal ERK1/2 and estrogen receptor alpha (ERalpha) phosphorylation signals. Endocrinology. 2011; 152:1434–47. [PubMed: 21303939]
31. El-Mas MM, Abdel-Rahman AA. Nongenomic effects of estrogen mediate the dose-related myocardial oxidative stress and dysfunction caused by acute ethanol in female rats. American journal of physiology Endocrinology and metabolism. 2014; 306:E740–7. [PubMed: 24368668]
32. Yao F, Abdel-Rahman AA. Estrogen Receptors alpha and beta Play Major Roles in Ethanol-Evoked Myocardial Oxidative Stress and Dysfunction in Conscious Ovariectomized Rats. Alcohol Clin Exp Res. 2016
33. Marcondes FK, Miguel KJ, Melo LL, Spadari-Bratfisch RC. Estrous cycle influences the response of female rats in the elevated plus-maze test. Physiology & behavior. 2001; 74:435–40. [PubMed: 11790402]
34. Hsieh YC, Choudhry MA, Yu HP, Shimizu T, Yang S, Suzuki T, et al. Inhibition of cardiac PGC-1alpha expression abolishes ERbeta agonist-mediated cardioprotection following trauma-hemorrhage. FASEB journal: official publication of the Federation of American Societies for Experimental Biology. 2006; 20:1109–17. [PubMed: 16770010]
35. Lu CLH, JC, Dun NJ, Oprea TI, Wang PS, Luo JC, Lin HC, Chang FY, Lee DD. Estrogen rapidly modulates 5-Hydroxytrtophan-induced visceral hypersensitivity via GPR30 in rats. Gastoenterology. 2009; 137:1040–50.
36. Wang X, Abdel-Rahman AA. Effect of chronic ethanol administration on hepatic eNOS activity and its association with caveolin-1 and calmodulin in female rats. American journal of physiology Gastrointestinal and liver physiology. 2005; 289:G579–85. [PubMed: 15845868]
37. Shaikh SR, Rockett BD, Salameh M, Carraway K. Docosahexaenoic acid modifies the clustering and size of lipid rafts and the lateral organization and surface expression of MHC class I of EL4 cells. The Journal of nutrition. 2009; 139:1632–9. [PubMed: 19640970]
38. Bolte S, Cordelieres FP. A guided tour into subcellular colocalization analysis in light microscopy. Journal of microscopy. 2006; 224:213–32. [PubMed: 17210054]
39. Collin B, Busseuil D, Zeller M, Perrin C, Barthez O, Duvillard L, et al. Increased superoxide anion production is associated with early atherosclerosis and cardiovascular dysfunctions in a rabbit model. Molecular and cellular biochemistry. 2007; 294:225–35. [PubMed: 16871360]
40. Yao F, Abdel-Rahman AA. Estrogen receptor ERalpha plays a major role in ethanol-evoked myocardial oxidative stress and dysfunction in conscious female rats. Alcohol. 2016; 50:27–35. [PubMed: 26695589]
41. Prisby RD, Dominguez JM 2nd, Muller-Delp J, Allen MR, Delp MD. Aging and estrogen status: a possible endothelium-dependent vascular coupling mechanism in bone remodeling. PLoS One. 2012; 7:e48564. [PubMed: 23185266]
42. Pearson K. Notes on regression and inheritance in the case of two parents. Proceedings of the Royal Society of London. 1895; 58:240–2.
43. Sosa L, Gutierrez S, Petiti JP, Palmeri CM, Mascanfroni ID, Soaje M, et al. 17beta-Estradiol modulates the prolactin secretion induced by TRH through membrane estrogen receptors via PI3K/Akt in female rat anterior pituitary cell culture. American journal of physiology Endocrinology and metabolism. 2012; 302:E1189–97. [PubMed: 22354782]

Author Manuscript Author Manuscript Author Manuscript Author Manuscript

44. Kocanova S, Mazaheri M, Caze-Subra S, Bystricky K. Ligands specify estrogen receptor alpha nuclear localization and degradation. BMC Cell Biol. 2010; 11:98. [PubMed: 21143970]
45. Sheldahl LC, Shapiro RA, Bryant DN, Koerner IP, Dorsa DM. Estrogen induces rapid translocation of estrogen receptor beta, but not estrogen receptor alpha, to the neuronal plasma membrane. Neuroscience. 2008; 153:751–61. [PubMed: 18406537]
46. Razandi M, Pedram A, Merchenthaler I, Greene GL, Levin ER. Plasma membrane estrogen receptors exist and functions as dimers. Molecular endocrinology. 2004; 18:2854–65. [PubMed: 15231873]
47. Lindberg MK, Moverare S, Skrtic S, Gao H, Dahlman-Wright K, Gustafsson JA, et al. Estrogen receptor (ER) -beta reduces ERalpha-regulated gene transcription, supporting a “ying yang” relationship between ERalpha and ERbeta in mice. Molecular endocrinology. 2003; 17:203–8. [PubMed: 12554748]
48. Liu MM, Albanese C, Anderson CM, Hilty K, Webb P, Uht RM, et al. Opposing action of estrogen receptors alpha and beta on cyclin D1 gene expression. The Journal of biological chemistry. 2002; 277:24353–60. [PubMed: 11986316]
49. Vivacqua A, Bonofiglio D, Recchia AG, Musti AM, Picard D, Ando S, et al. The G protein-coupled receptor GPR30 mediates the proliferative effects induced by 17beta-estradiol and hydroxytamoxifen in endometrial cancer cells. Molecular endocrinology. 2006; 20:631–46. [PubMed: 16239258]
50. Shaikh SR, Edidin MA. Membranes are not just rafts. Chemistry and physics of lipids. 2006; 144:1–3. [PubMed: 16945359]
51. Griendling KK, Touyz RM, Zweier JL, Dikalov S, Chilian W, Chen YR, et al. Measurement of Reactive Oxygen Species, Reactive Nitrogen Species, and Redox-Dependent Signaling in the Cardiovascular System: A Scientific Statement From the American Heart Association. Circulation research. 2016; 119:e39–75. [PubMed: 27418630]
52. Campos C, Casali KR, Baraldi D, Conzatti A, Araujo AS, Khaper N, et al. Efficacy of a low dose of estrogen on antioxidant defenses and heart rate variability. Oxidative medicine and cellular longevity. 2014; 2014:218749. [PubMed: 24738017]
53. Nadal-Serrano M, Sastre-Serra J, Pons DG, Miro AM, Oliver J, Roca P. The ERalpha/ERbeta ratio determines oxidative stress in breast cancer cell lines in response to 17beta-estradiol. Journal of cellular biochemistry. 2012; 113:3178–85. [PubMed: 22615145]
54. Miro AM, Sastre-Serra J, Pons DG, Valle A, Roca P, Oliver J. 17beta-Estradiol regulates oxidative stress in prostate cancer cell lines according to ERalpha/ERbeta ratio. The Journal of steroid biochemistry and molecular biology. 2011; 123:133–9. [PubMed: 21172438]
55. Barp J, Sartorio CL, Campos C, Llesuy SF, Araujo AS, Bello-Klein A. Influence of ovariectomy on cardiac oxidative stress in a renovascular hypertension model. Canadian journal of physiology and pharmacology. 2012; 90:1229–34. [PubMed: 22900708]
56. Ceravolo GS, Filgueira FP, Costa TJ, Lobato NS, Chignalia AZ, Araujo PX, et al. Conjugated equine estrogen treatment corrected the exacerbated aorta oxidative stress in ovariectomized spontaneously hypertensive rats. Steroids. 2013; 78:341–6. [PubMed: 23261957]
57. Myers CL, Weiss SJ, Kirsh MM, Shepard BM, Shlafer M. Effects of supplementing hypothermic crystalloid cardioplegic solution with catalase, superoxide dismutase, allopurinol, or deferoxamine on functional recovery of globally ischemic and reperfused isolated hearts. The Journal of thoracic and cardiovascular surgery. 1986; 91:281–9. [PubMed: 3945095]
58. Lagranha CJ, Deschamps A, Aponte A, Steenbergen C, Murphy E. Sex differences in the phosphorylation of mitochondrial proteins result in reduced production of reactive oxygen species and cardioprotection in females. Circulation research. 2010; 106:1681–91. [PubMed: 20413785]

Author Manuscript Author Manuscript Author Manuscript Author Manuscript

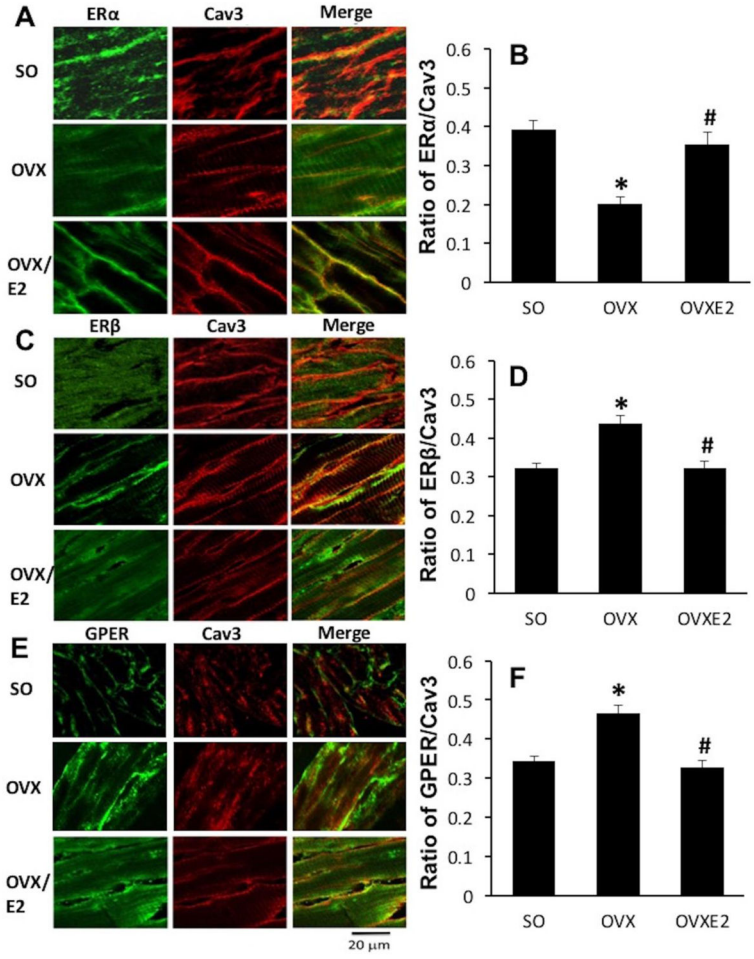

Figure 1.

Acute E_2 (1 μg/kg i.v., OVXE2) enhances ERα, but reduces ERβ and GPER, localization at the cardiac myocyte plasma membrane of ovariectomized (OVX) rats to comparable levels of sham-operated (SO) rats. **A, C and E** show representative confocal images of rat heart sections with ERα, ERβ or GPER-FITC (green) and Cav3-Cy3 (red) antibodies. Merged images highlight ERs and Cav3 colocalization (yellow). The bar graphs summarized the ratio of membrane ERα, ERβ or GPER vs Cav3, respectively (**B, D and F**). Values are mean ± SEM of 4–5 hearts. *$P < 0.05$ vs SO, #$P < 0.05$ vs OVX.

Author Manuscript Author Manuscript Author Manuscript Author Manuscript

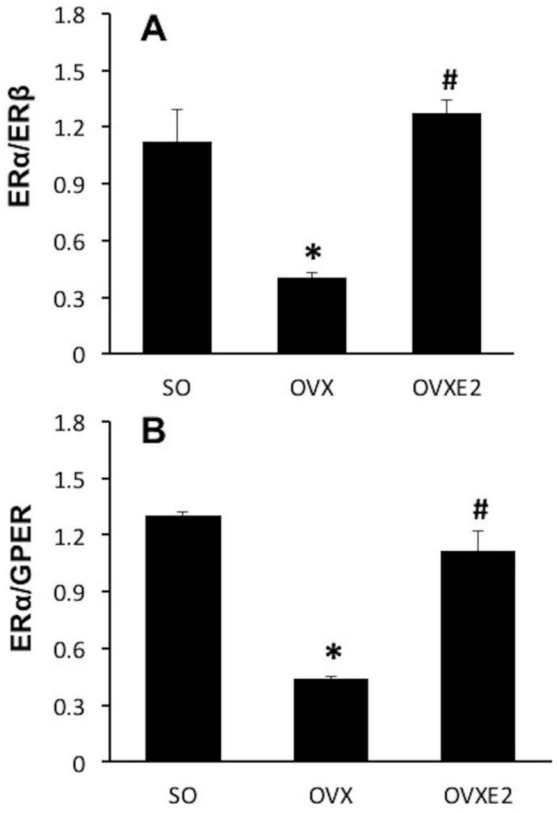

Figure 2.

ERα vs ERβ (**A**) and GPER (**B**) ratios at the cardiac myocyte plasma membrane in sham-operated (SO) and ovariectomized (OVX) rats and OVX rats pretreated with acute E_2 (1 μg/kg i.v., $OVXE_2$). Values are mean ± SEM of 4–5 hearts. *$P < 0.05$ vs SO, #$P < 0.05$ vs OVX.

Author Manuscript Author Manuscript Author Manuscript Author Manuscript

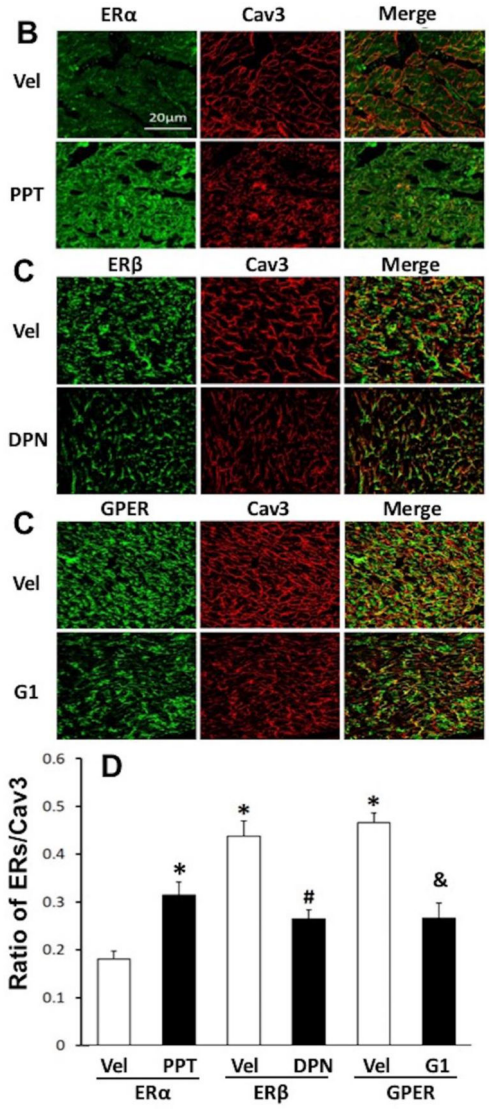

Figure 3.

Selective ERα agonist PPT enhances ERα, while ERβ and GPER agonist DPN and G1 (10 μg/kg, i.v., each) reduces ERβ and GPER, localization at the cardiac myocyte plasma membrane of ovariectomized (OVX) rats. **A, B and C** show the representative confocal images of PPT, DPN and G1 or vehicle-treated rat heart sections with ERα, ERβ or GPER-FITC (green) and Cav3-Cy3 (red) antibodies. Merged images highlight ERs and Cav3 colocalization (yellow). The bar graphs summarized the ratio of membrane ERα, ERβ or GPER vs Cav3 (**D**). Values are mean ± SEM of 4–5 hearts. *$P < 0.05$ vs ERα-Veh, #$P < 0.05$ vs ERβ-Veh, &$P < 0.05$ vs GPER -Veh.

Author Manuscript Author Manuscript Author Manuscript Author Manuscript

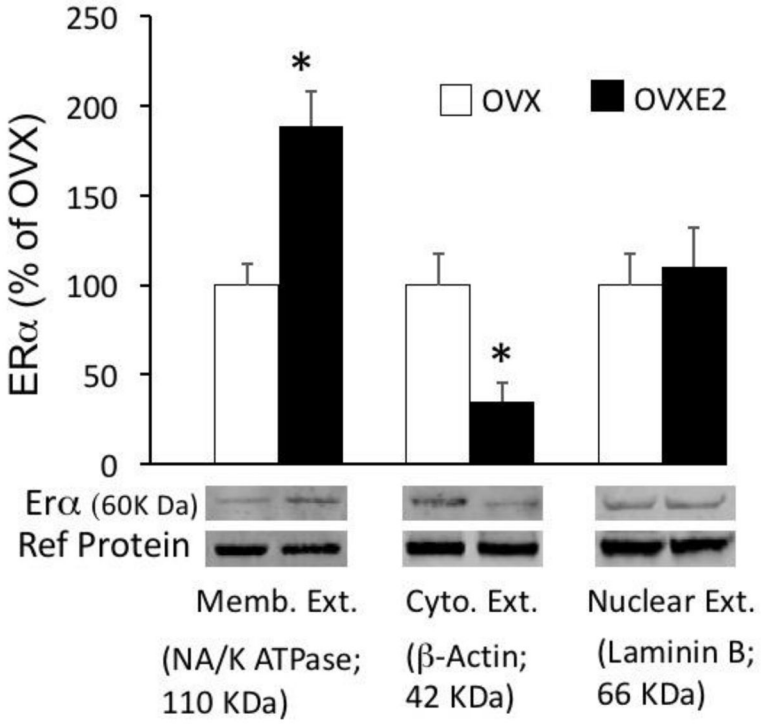

Figure 4.

ERα protein level in membrane fraction extracts (ME) was increased, while reduced in cytoplasmic fraction extracts (CE) by acute E_2 ($OVXE_2$, 1 μg/kg) treatment in OVX rat myocardial tissues. Levels of ERα protein in nuclear extracts (NE) were not changed. The amount of ERα protein level in ME, CE and NE represents mean band intensity normalized to NA/K ATPase, beta actin and Laminin B, respectively, and expressed as % of OVX (saline) values. Values are mean ± SEM of 4 hearts. *$P < 0.05$ vs OVX-ME, #$P < 0.05$ vs OVX-CE.

Author Manuscript Author Manuscript Author Manuscript Author Manuscript

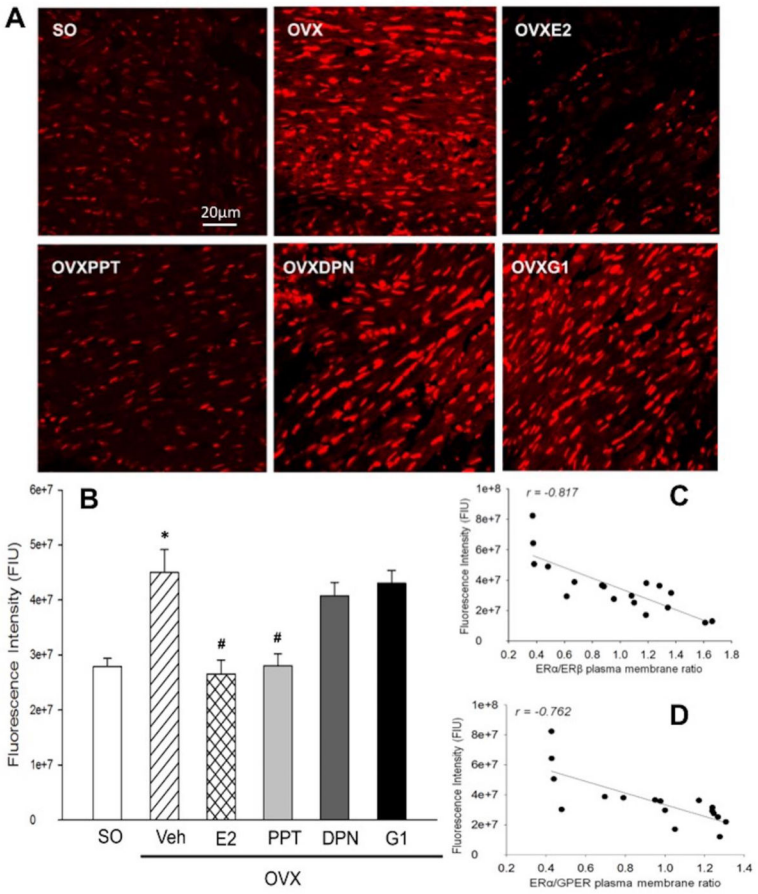

Figure 5.

The effect of ER activation/translocation on myocardial reactive oxygen species (ROS). (**A**) Representative myocardial sections showing ROS level indicated by dihydroethidium (DHE) staining (red) in sham operated (SO) and in ovariectomized (OVX) rats treated with estrogen (1μg/kg i.v.; $OVXE_2$), saline (OVX), or selective ER agonists (10 μg/kg i.v.; OVXPPT, OVXDPN or OVXG1). (**B**) Bar graph is showing the effect of estrogen receptor activation on ROS level expressed as mean fluorescence intensity (FIU) of DHE staining measured using NIH ImageJ analysis of confocal images. Inverse relationship between ERα/ERβ (**C**) or ERα/GPER (**D**) OVX and $OVXE_2$ ratios at the cardiac myocytes plasma membrane and myocardial ROS levels. Values are mean ± SEM. *$P < 0.05$ vs SO, #$P < 0.05$ vs OVX-Vel.

Author Manuscript Author Manuscript Author Manuscript Author Manuscript

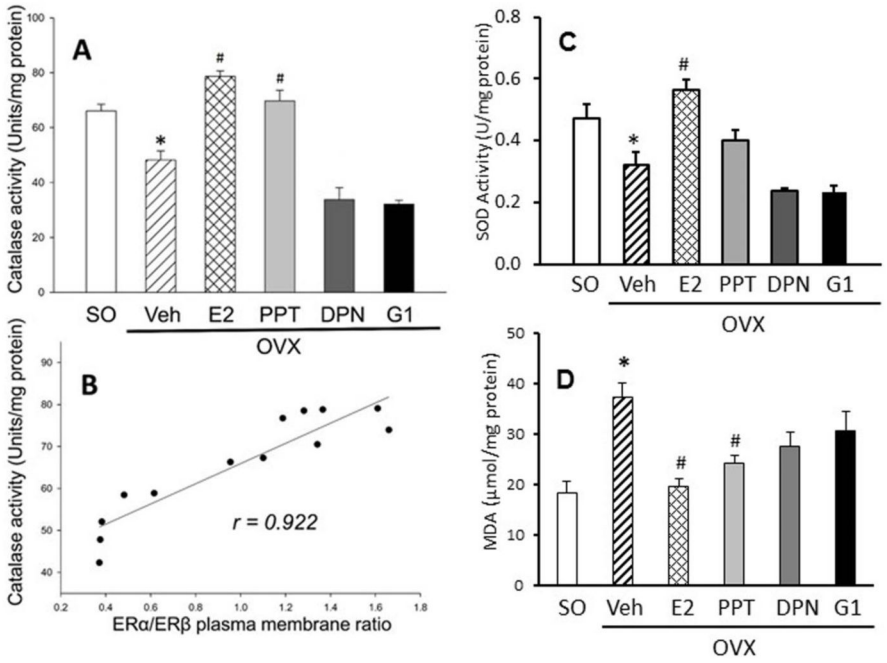

Figure 6.

Estrogen increased the ERα/ERβ ratio at the myocytes plasma membrane as well as myocardial catalase and superoxide dismutase (SOD) activities while reducing malondialdehyde (MDA) in OVX rats' hearts. Cardiac tissues were obtained from sham-operated (SO) or ovariectomized (OVX) rats pretreated with acute E_2 (1 μg/kg i.v., $OVXE_2$), selective ERα (PPT), ERβ (DPN), GPER (G1) agonists (10 μg/kg, each), or saline (OVX). Scatter plots revealed positive correlation ($P < 0.05$) between ERα/ERβ ratios at plasma membrane and catalase activity in the myocardium of OVX and $OVXE_2$ rat (**B**). A similar correlation existed between or ERα/GPER ration and catalase activity (not shown). Values are mean ± SEM of 5–6 hearts. *$P < 0.05$ vs SO, #$P < 0.05$ vs OVX-Veh.

Author Manuscript Author Manuscript Author Manuscript Author Manuscript

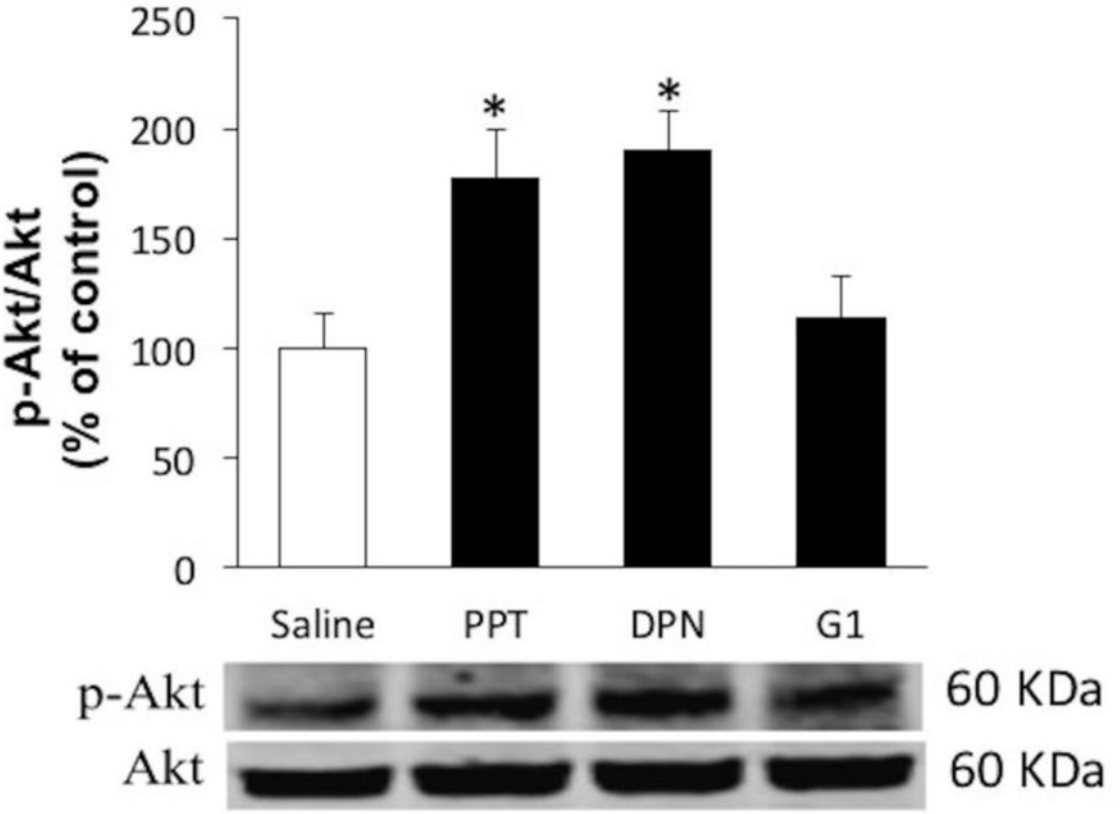

Figure 7.

The effect of individual ER activation on myocardial Akt phosphorylation in OVX rats. The phosphorylation level of myocardial Akt in OVX rats treated with selective ERα (PPT), ERβ (DPN), GPER (G1) agonist (10 μg/kg) or saline was determined by Western blot. Phosphorylation level of Akt is presented as the ratio of phosphorylated (p-Akt) to total Akt (Akt) and normalized to the corresponding level in saline-treated OVX (control) rats. The images under the bar graph are the representative bands of p-Akt and Akt. Values are mean ± SEM. *$P < 0.05$ vs control (saline) group.